

Software for automatic calibration of synchrotron powder diffractometers

David Laundy,* Chiu Tang, Mark Roberts, Mike Miller, Stephen Thompson and Graham Bushnell-Wye

Daresbury Laboratory, Warrington, Cheshire WA4 4AD, UK.
E-mail: d.laundy@dl.ac.uk

An automatic procedure to calibrate angular-dispersive monochromatic diffraction instruments has been developed at the Daresbury Synchrotron Radiation Source. The procedure uses a macro language to control the powder diffraction instruments to locate Bragg reflections and perform peak-centre refinement from a standard reference material. The information obtained is used to refine the wavelength of the radiation used and the angular offset of the detector arm. The concept and implementation of the new software are described with applications to demonstrate its viability. The results of a reliability and accuracy study are also presented.

Keywords: synchrotron X-rays; powder diffraction; instrument calibration.

1. Introduction

1.1. Diffraction instruments

There are two angular-dispersive powder diffraction instruments at the SRS, Daresbury Laboratory, namely stations 2.3 and 9.1. These stations receive a high flux of white X-ray beam from the 2 GeV synchrotron. The instruments were initially built for high-resolution diffraction studies, and they are now used for routine structural analysis of polycrystalline specimens in powder form. Instrumental details can be found in previous publications (Bushnell-Wye & Cernik, 1992; Collins *et al.*, 1992). Briefly, each station consists of a channel-cut monochromator (silicon single-crystal) which filters the white radiation giving a beam of fixed wavelength and a diffractometer which collects the scattered X-rays from the powder specimen. The diffractometer operates by scanning a detector mounted on a 2θ -circle through a range of angles, at a fixed step size, around the sample. The use of parallel foils and flat-plate sample (Hart–Parrish geometry) is one of the two main diffraction configurations. High collimation of the diffracted beam is achieved through a set of long parallel foils with an aperture of approximately 20×20 mm attached onto the 2θ arm. The foils assembly is constructed by stacking 80 thin foils, each of length 355 mm, spaced 0.2 mm apart, to define a nominal acceptance angle of 0.06° . A set of short vertical foils with an acceptance angle of 1° are used to reduce axial divergence and improve the peak symmetry at low detector angles. Detailed technical descriptions and collimation performance of the foils can be found in the work of Roberts & Tang (1998). In the other configuration (Debye–Scherrer geometry), the parallel foils are replaced by two pairs of well separated single slits to provide the diffraction collimation (MacLean *et al.*, 2000). The flat-plate sample is replaced by a capillary specimen placed at the centre of the diffractometer.

1.2. Calibration objective

These stations are multipurpose instruments with several scattering geometries available to satisfy a diverse user community; thus a change of configuration is often practised. Although the mechanism

to clamp the collimation hardware does provide stability, there is no guarantee that the slits or the parallel foils will return to exactly the same position. In order to collect and to analyse the diffraction from a sample, it is necessary to know the angle offset of the detector, *i.e.* the actual 2θ -arm angle relative to the incident X-ray beam. The double-bounce monochromator crystal is mounted on a rotary table which allows the angle to be changed to select the required X-ray wavelength. Although the 2θ -arm circle and the monochromator rotary table are extremely accurate and stable ($\pm 0.0001^\circ$), they have no absolute angle calibration, and so for a measurement the position of each is uncertain to within an unknown offset. The two unknown offsets must be determined before a measurement can proceed. This is most easily done by replacing the sample with a standard reference powder and performing a calibration experiment. The calibration procedure can be performed manually with the user first selecting a number of reflections and setting up scans on each reflection. The data from each scan would then be input into a peak-fitting program to locate the centre of each peak, and then the peak centres and the reflection indices would be fed into another program which refined the wavelength and detector-arm offset. However, this procedure is lengthy, labour intensive and prone to mistakes. With the introduction of new station control software, the calibration was automated.

2. Control software

Each station is controlled by a PC running Windows NT. The data-acquisition hardware is accessed through a CAMAC crate with associated controller that is connected *via* an IEEE488 interface or proprietary ISA bus card. Other devices may also be connected, for example to the PC COM Ports, PCI bus or *via* Ethernet. The data-acquisition software is the *PINCER* program developed at Daresbury Laboratory (Oszlanyi & Miller, 1992; Miller *et al.*, 1994). With further developments (Miller *et al.*, 1998), the software is now used on all our diffraction stations. The *PINCER* data-acquisition program provides a command language interpreter with a tool kit of portable data-acquisition and support functions that can be invoked interactively or from macro command files. Internal variable handling, screen and file input/output, maths functions, hardware input/output, graphics and flow control are supported. More recently, *PINCER* has been enhanced to allow run-time linking with windows dynamic link and static libraries using a generic interface for greater flexibility and extensibility. On the stations, a set of macros, the PD (powder diffraction) macro set, runs under *PINCER* and this gives a menu-driven interface to a set of powerful functions that allow the user to drive motors (both real and virtual), perform scans to collect data and to align the station.

3. Methodology

3.1. Standard reference sample

The standard reference powder most commonly used for the calibration is silicon which gives sharp diffraction peaks at well known positions. At Daresbury, a silicon powder prepared by the National Institute of Standards and Technology (NBS SRM640b) is used for this purpose. This material has been extensively characterized previously (Rasberry, 1987) and has a cubic structure with space group $Fd\bar{3}m$, and the accepted lattice parameter is 357.0940 (35) Å. It is necessary that the X-ray wavelength (λ) and the detector-arm offset ($2\theta_0$) are known approximately at the start of the procedure so that the reflections can be initially identified and located. This can be done sufficiently accurately by using an optical leveller to align the monochromator crystal and a spirit level for the detector arm.

3.2. Program requirements and the algorithm

The following was required of the program:

- (i) the program should be robust, it should recover from loss of the X-ray beam and the numerical routines should be stable;
- (ii) the calibration should be accurate;
- (iii) the program should be optimized for minimal loss of time – no significant delay for the calculation using the interpreted command language;
- (iv) it should be possible to re-calibrate the monochromator and the detector-arm angle from within the *PINCER* program;
- (v) the program should be easy to use – sensible default values should be provided for all input parameters;
- (vi) unattended operation mode when the program uses default values and does not require user input should be possible;
- (vii) data including accurate scans of powder peaks and the final calibration should be recorded;
- (viii) the program should not assume a particular profile shape for the powder peaks so that it can be used with different experimental geometries and different calibration samples.

The calibration process consists of two main tasks. The first task is to scan a diffraction peak known to lie within a given 2θ angular range and to determine, from the scan data, the peak position. The second task is to use the peak positions of a number of reflections and the indices (hkl) of each reflection to calculate the wavelength and detector-arm calibration. Except at very low angles where axial divergence causes peak asymmetry, the diffraction peaks are symmetric and the peak position can be defined in a number of equivalent ways, for example as the position of maximum intensity or as the position of the centroid of the peak. The peak position may be determined by fitting a model peak function to the data but this requires a good model function which may have to vary with the experimental geometry. The method adopted here is to calculate the peak centroid directly from the experimental data.

3.3. Scan ranges and peak locations

The centroid of a peak with intensity $p(\theta)$ is defined as

$$m = \frac{\int_{-\infty}^{+\infty} \theta p(\theta) d\theta}{\int_{-\infty}^{+\infty} p(\theta) d\theta}. \quad (1)$$

In order to find the peak centroid, the powder intensity is measured as the sample angle θ and detector angle 2θ are scanned with a small step through the peak. The scan range must, however, be finite and so the limits in the integrals in equation (1) must therefore be replaced by finite limits. In addition, finite step size means that the integrals are approximated as summations over the discrete θ angles; however, by taking a small step size we can ensure that the difference is negligible. The intensity of a powder peak centred at θ_C can be written as $p(\theta) = f(\theta - \theta_C)$. We assume that the peak is symmetrical so that $f(\theta) = f(-\theta)$ and therefore $\int_{-L}^{+L} \varphi f(\varphi) d\varphi = 0$.

If the initial estimated centre of the peak is at an angle $\theta_C + \omega$, *i.e.* offset by an angle ω from the actual peak centre, and if the total scan range is δ , then the scan range is from $\theta_C + \omega - \delta/2$ to $\theta_C + \omega + \delta/2$. Using these values as the limits of the integrals to calculate the centroid, the new estimated peak position can be written as

$$\begin{aligned} \theta_P &= \frac{\int_{\theta_C + \omega - \delta/2}^{\theta_C + \omega + \delta/2} \theta f(\theta - \theta_C) d\theta}{\int_{\theta_C + \omega - \delta/2}^{\theta_C + \omega + \delta/2} f(\theta - \theta_C) d\theta} = \frac{\int_{\omega - \delta/2}^{\omega + \delta/2} (\theta_C + \varphi) f(\varphi) d\varphi}{\int_{\omega - \delta/2}^{\omega + \delta/2} f(\varphi) d\varphi} \\ &= \theta_C + \frac{\int_{\omega - \delta/2}^{\omega + \delta/2} \varphi f(\varphi) d\varphi}{\int_{\omega - \delta/2}^{\omega + \delta/2} f(\varphi) d\varphi}. \quad (2) \end{aligned}$$

The difference between the estimated and the true peak position is $\Delta\theta_P = \theta_P - \theta_C$ which can be obtained from equation (2),

$$\begin{aligned} \Delta\theta_P &= \frac{\int_{\omega - \delta/2}^{\omega + \delta/2} \varphi f(\varphi) d\varphi}{\int_{\omega - \delta/2}^{\omega + \delta/2} f(\varphi) d\varphi} \\ &= \frac{\int_{-\delta/2}^{+\delta/2} \varphi f(\varphi) d\varphi + \int_{\omega - \delta/2}^{-\delta/2} \varphi f(\varphi) d\varphi + \int_{\delta/2}^{\omega + \delta/2} \varphi f(\varphi) d\varphi}{\int_{-\delta/2}^{+\delta/2} f(\varphi) d\varphi + \int_{\omega - \delta/2}^{-\delta/2} f(\varphi) d\varphi + \int_{\delta/2}^{\omega + \delta/2} f(\varphi) d\varphi}. \quad (3) \end{aligned}$$

In equation (3), the first term in the numerator is zero because the peak is symmetrical and the limits of the integral are symmetrical about $\varphi = 0$. The first term in the denominator is the normalization of the peak over the centred scan range which we can call N . The remaining integrals in the numerator can be evaluated by using the symmetry of $f(\varphi)$ to combine the two integrals,

$$\begin{aligned} \int_{\omega - \delta/2}^{-\delta/2} \varphi f(\varphi) d\varphi + \int_{\delta/2}^{\omega + \delta/2} \varphi f(\varphi) d\varphi &= \int_{\delta/2 - \omega}^{\delta/2} \varphi f(\varphi) d\varphi + \int_{\delta/2}^{\delta/2 + \omega} \varphi f(\varphi) d\varphi \\ &= \int_{\delta/2 - \omega}^{\delta/2 + \omega} \varphi f(\varphi) d\varphi, \end{aligned}$$

and then, if the scan is close to being centred on the peak so that ω is small, $f(\varphi)$ can be considered as constant over the range of the integral, so

$$\begin{aligned} \int_{\delta/2 - \omega}^{\delta/2 + \omega} \varphi f(\varphi) d\varphi &\simeq \int_{\delta/2 - \omega}^{\delta/2 + \omega} \varphi f(\delta/2) d\varphi \\ &= f(\delta/2) \int_{\delta/2 - \omega}^{\delta/2 + \omega} \varphi d\varphi \\ &= \omega \delta f(\delta/2). \end{aligned}$$

A similar argument can be used to show that the second and third term in the denominator of equation (3) cancel to give the final result for the error in θ_P ,

$$\Delta\theta_P \simeq \omega \delta f(\delta/2)/N. \quad (4)$$

This term will be zero if the scan range is centred on the peak ($\omega = 0$); however, as mentioned before, a centred scan range cannot be chosen before the peak position is known. In Fig. 1, the factor $\delta f(\delta/2)/N$ in equation (4) is plotted against the total scan range, δ , for a silicon 220 reflection measured on station 2.3. This shows that, for this peak, if the scan range is about 0.15° , the error in determining the peak position will be about 15% of the error in the centring of the scan on the peak. If the scan range is made larger than this, there will be only

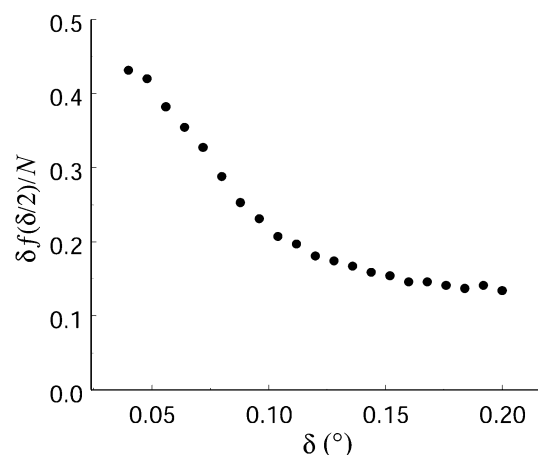


Figure 1 Variation in error term $\delta f(\delta/2)/N$ with the scan range δ .

Table 1

The calibration macros and their function.

Macro name	Function
sicalib	Top level main macro. Performs refinement for silicon powder sample.
hklfcc	Calculates the reflection indices for the first n reflections of crystals of silicon structure.
refine	The main refinement macro – sets up scan ranges. Calls scan macro, and the macro to refine wavelength and $2\theta_0$ position. Writes the data to the log file.
hklpeak	Calculates the scan start position, end position and step for the i th peak given an estimated peak position and scan range.
smain	Main scan macro from the PD macro set.
calibfit	Performs the wavelength and $2\theta_0$ refinement using the Newton–Raphson method.

a small reduction in the error and the required scan time will be increased. The peak position can be determined by iteration, using the measured peak position from one scan to determine the scan ranges for the next scan. The initial scan ranges depend on the initial calibration of λ and θ_0 which are used to predict the peak positions using Bragg's law and the initial range must be large enough to ensure that the peak is covered. After the initial scan, a scan range of 0.2° was chosen. After station reconfiguration, the initial estimated peak positions can be in error by as much as 0.5° which leads to peak-position errors of up to about 0.1° . Test measurements show, however, that after the iteration process the peak-position error is less than 0.001° .

3.4. Wavelength and 2θ refinement

The powder peak positions are related to the wavelength of the radiation by Bragg's law. Given a measurement of two or more peak positions using the above method, the wavelength and 2θ offset angle are determined using a macro which implemented the Newton and Raphson method. The method proceeds by iteration until the corrections to λ and θ_0 fall below some cut-off level. Close to the solution, the Newton–Raphson method converges quadratically and so the cut-off levels can be chosen to be small with little increase in computation time (*e.g.* $\Delta\lambda/\lambda = 10^{-6}$ and $\Delta\theta_0 = 10^{-6}$ rad).

The calibration procedure is as follows:

(i) the two strongest peaks ($i = 1$ and $i = 2$), 111 and 220 reflections in the case of a silicon powder, are scanned using wide scan ranges and large step sizes to obtain the peak positions approximately – these are used to refine λ and θ_0 ;

(ii) these first two peaks are then scanned again, using narrower scan ranges, smaller step sizes and now with better centring of the scan ranges about each peak so that the error in obtaining the peak position is reduced. Once again λ and θ_0 are refined obtaining more accurate values;

(iii) finally, the n peaks are scanned in order with the well centred scan ranges. After scanning the second and each subsequent peak, the peak positions are used to further refine λ and θ_0 .

4. The calibration macros

The calibration macros consist of a main macro, sicalib.mac, which is called from the command line or may be called from a batch macro. This macro calls other macro, as summarized in Table 1. The macros can run unattended and then default values are used for the input parameters. In the interactive mode of operation, the macros request that the user inputs a monochromator angle discrepancy and a $2\theta_0$ angle discrepancy which are the maximum allowed calibration offsets. These are used to set up the initial scan ranges to ensure that the

Table 2

An example of the calibration using the capillary geometry on station 9.1.

REFINE:	1	1	1	fit = 18.2889	del = -0.0017
REFINE:	2	2	0	fit = 30.0834	del = -0.0000
REFINE:	3	1	1	fit = 35.4340	del = 0.0010
REFINE:	4	0	0	fit = 43.0638	del = 0.0005
REFINE:	3	3	1	fit = 47.1501	del = 0.0015
REFINE:	4	2	2	fit = 53.4238	del = 0.0004
REFINE:	3	3	3	fit = 56.9495	del = 0.0001
REFINE:	4	4	0	fit = 62.5362	del = -0.0005
REFINE:	5	3	1	fit = 65.7528	del = -0.0007
REFINE:	6	2	0	fit = 70.9444	del = -0.0007
REFINE:	5	3	3	fit = 73.9801	del = -0.0006
REFINE:	4	4	4	fit = 78.9432	del = 0.0006
REFINE:	Refined wavelength = 0.996608 Å				
REFINE:	Refined $2\theta_0 = 0.006727^\circ$				

peaks are within range. The default values are 0.002° for the monochromator angle and 1° for the 2θ arm. The program also asks for the number of peaks to be scanned (default is nine peaks) and the counting time per point (default is 1 s). At the end of the calibration, in interactive mode the user is asked whether the monochromator angle and the 2θ -arm angle should be re-calibrated by the macro. The peak scan data and the refinement results are written to the log file.

5. Application and accuracy

Initially, the angle of the Si(111) crystal is positioned to an intended wavelength using the PD 'mono' macro. Often, the wavelength with the maximum X-ray flux is chosen by the user, typically $\lambda = 1.0$ Å and 1.4 Å for stations 9.1 and 2.3, respectively. Using the default parameters described in the previous section, the entire calibration only takes approximately 20 min to complete. Table 2 shows a typical log file output from the refinement taken on station 9.1 using the Debye–Scherrer configuration. For each peak, the reflection indices are shown, followed by the peak position ('fit =') in degrees and the discrepancy from the refined position ('del =') in degrees. At the end of the macro, the wavelength in angstroms and $2\theta_0$ position in degrees are recorded in the log file. The refined values for λ and zero point are highlighted in bold. Similarly, the main macro was applied on station 2.3 using the Hart–Parrish geometry. As an example, a refinement using nine reflections yielded $\lambda = 1.399727$ (2) Å and $2\theta_0 = -0.00038$ (11) $^\circ$. Subsequently the pattern was measured using the conventional $\theta/2\theta$ scan for Le Bail refinement (Le Bail, 1992). The scan step used was 0.005° with 2 s per point. The measurement took several hours to be completed and is shown in Fig. 2. A good refinement (solid line in the figure) was obtained using the same lattice parameter of silicon. The Bragg peaks labelled were fitted with the appropriate profile function (pseudo-Voigt). The refined zero point is -0.00031 (4) $^\circ$. The angular parameter is expected to be very close to zero since the control computer was previously instructed that the two parameters be calibrated after the completion of the initial run. A slightly bigger λ of 1.399735 Å was also obtained in the refinement. The small wavelength drift (8×10^{-6} Å) and angular offset (0.00007°) are, however, within the level of beam stability discussed later.

In addition to the refinement of λ and $2\theta_0$, the macros can be used to monitor the SRS beam stability or instrument performance by running a number of calibrations in succession. In Fig. 3 the results of λ (*a*) and zero points (*b*) are shown, obtained after 39 refinements (~ 15 h) on station 2.3. The gap in the measurements occurred when the beam was interrupted for a refill of the synchrotron. The standard deviation of the λ distribution is small ($\Delta\lambda = \pm 1 \times 10^{-5}$ Å) and is even smaller if data from after the refill is used ($\Delta\lambda = \pm 0.4 \times$

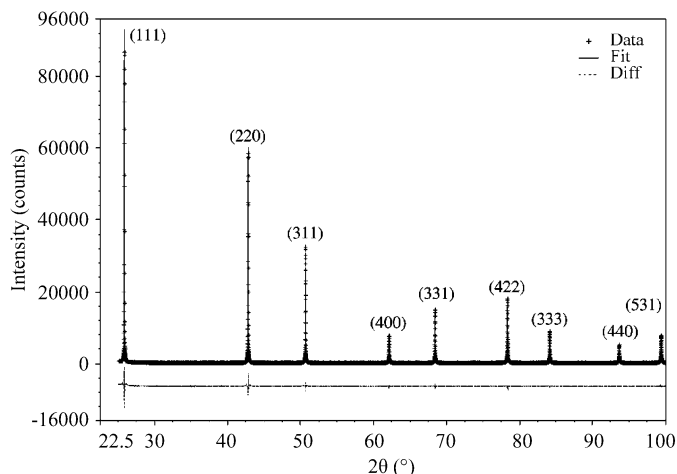


Figure 2
The silicon powder pattern: the presence of the first nine Bragg peaks with their hkl labelled. The experimental points are shown as crosses and the data from the Le Bail refinement (see text) are shown as the solid line.

10^{-5} Å). The average value of λ is 1.399950 Å with the smallest and largest values being 1.399936 and 1.399956 Å, respectively. Similarly, the standard deviation of the 2θ distribution is also small ($\pm 0.0003^\circ$). The average value is 0.0009° with a minimum of 0.0006° and a maximum of 0.0012° . The application of the macro in this way has proved to be a useful exercise, giving an indication of the stability of the instrument.

6. Conclusion

When the station software was upgraded to the *PINCER* command language, the calibration procedure was automated. The procedure is very user-friendly allowing calibration to be performed routinely on the powder diffraction stations. The calibration refinements, λ value and $2\theta_0$ position are displayed on screen. These results and other detailed information are logged allowing the users to check the confidence of the actual calibration. The requirements initially specified have been fully met by the macros. The new method compares well with the previous calibration method which involved a lengthy peak-fitting procedure followed by transfer of the data into a refinement program. In addition, the new software is a useful tool to routinely monitor instrument performance and SRS beam stability. The small distributions in the wavelength and $2\theta_0$ position showed the high accuracy of the refined calibration parameters, and the reliability of the procedure. The ease with which the diffraction instrument can

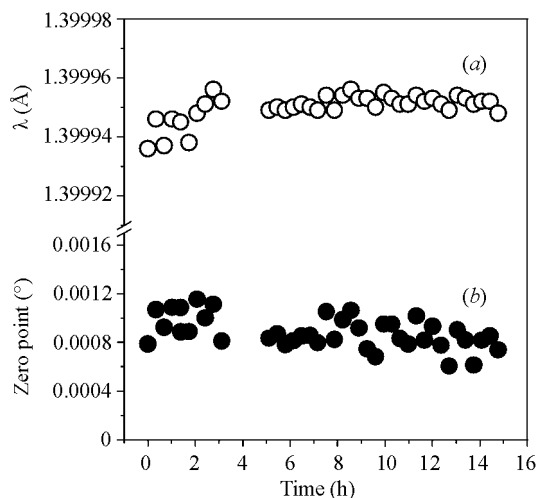


Figure 3
The results from the application of multiple calibration runs showing (a) wavelength (open circles) and (b) $2\theta_0$ point (solid circles) as a function of time. The average values and distributions for λ and $2\theta_0$ are stated in the text.

be calibrated allows greater flexibility in the use of the station and has made a significant saving in set-up time for the stations.

References

- Bushnell-Wye, G. & Cernik, R. J. (1992). *Rev. Sci. Instrum.* **63**, 999–1001.
- Collins, S. P., Cernik, R. J., Pattison, P., Bell, A. T. M. & Fitch, A. N. (1992). *Rev. Sci. Instrum.* **63**, 1013–1014.
- Le Bail, A. (1992). *Accuracy in Powder Diffraction II*, National Institute of Standards and Technology Special Publication 846, edited by E. O. Prince & J. K. Stalick, p. 213. Washington: US Department of Commerce.
- MacLean, E. J., Millington, H. F. F., Neild, A. A. & Tang, C. C. (2000). *Mater. Sci. Forum.* **321/324**, 212–217.
- Miller, M. C., Ackroyd, K. S. & Oszlanyi, G. (1994). Daresbury Preprint DL/CSE/P29E. Daresbury Laboratory, Daresbury, Warrington WA4 4AD, UK. (Presented at the 8th ESONE International Conference on Real-Time Data, Dubna, Russia, June 1994.)
- Miller, M. C., Oszlanyi, G., Ackroyd, K. S., Marshall, C., Collins, S. P., Laundy, D. & Cernik, R. J. (1998). *J. Appl. Cryst.* **31**, 972–973.
- Oszlanyi, G. & Miller, M. C. (1992). Daresbury Preprint DL/Sci/TM86E. Daresbury Laboratory, Daresbury, Warrington WA4 4AD, UK.
- Rasberry, R. D. (1987). Certificate of Analysis: SRM 640b, Silicon Powder $2\theta/d$ -Spacing Standard. National Institute of Standards and Technology, Gaithersburg, MD 20899, USA.
- Roberts, M. A. & Tang, C. C. (1998). *J. Synchrotron Rad.* **5**, 1270–1274.